American Mineralogist, Volume 73, pages 1267–1274, 1988

Stoichiometry of the iron oxidation reaction in silicate melts

V. C. Kress, I.S.E. Carmichael

Department of Geology and Geophysics, University of California at Berkeley, Berkeley, California 94720, U.S.A.

Abstract

Experiments have been performed that calibrate the stoichiometry and thermodynamics of the iron oxidation reaction in natural silicate melts. A series of experiments was carried out on six melt compositions covering a far larger range of oxygen fugacities than had been examined previously. Oxygen fugacities between air and 5.2 $\log_{10}$ units below those defined by the nickel–nickel oxide assemblage were investigated at 1360 °C and 1460 °C. Results of these experiments confirm that $\ln(X_{Fe_2O_3}/X_{FeO})$ is a linear function of $\ln f_{O_2}$ over this entire range, and that this linear behavior is independent of composition over the range considered. These results are inconsistent with an ideal mixing between FeO and Fe_2O_3 components. They are, however, entirely consistent with ideal mixing between FeO and $FeO_{1.464\pm0.003}$ ($FeO \cdot 6Fe_2O_3$) components. A second series of experiments was performed on a single mid-ocean ridge basalt composition (JDFD2) in order to better constrain the temperature dependence of the iron oxidation reaction in this simplified two-component subsystem. This series was carried out at temperatures between 1299 °C and 1636 °C in air, CO_2, and 0.2 $\log_{10}$ units below the fayalite-magnetite-quartz buffer assemblage. Results of both series of experiments were combined with the Sack et al. (1980) and Kilinc et al. (1983) databases to estimate thermodynamic parameters for the iron oxidation reaction expressed in terms of FeO and $FeO_{1.464}$ components. These coefficients offer the most precise method available for estimation of iron oxidation state in natural silicate melts as a function of $\ln f_{O_2}$, temperature, and composition. Our results support the conclusion (Christie et al., 1986) that mid-ocean ridge basalts (MORBs) equilibrate as much as 3 $\log_{10}$ units below that defined by the nickel–nickel oxide assemblage.

Introduction

Iron is unique among the major constituents of natural silicate melts in that it is present in significant portions in more than one oxidation state. The partitioning of iron between ferric and ferrous species can substantially influence differentiation trends in crystallizing silicate magmas. Further, because the ferric and ferrous cations play different structural roles in the melt, ferric-ferrous equilibrium may also have significant effect on silicate-melt properties such as density (Henderson et al., 1961; Dickamer et al., 1969; Mo et al., 1982; Bottinga et al., 1982, 1983; Lange and Carmichael, 1987) and viscosity (Densem and Turner, 1938; Cukierman and Uhlmann, 1974; Mysen et al., 1985b). Thus, the distribution of iron between ferric and ferrous species provides a means by which variations in the chemical potential of oxygen, a quite mobile species, can profoundly influence the structure, rheology, and chemical composition of an evolving magma.

The iron oxidation reaction in silicate melts is commonly expressed in terms of the reaction

$$2FeO^{melt} + \tfrac{1}{2}O_2^{gas} = Fe_2O_3^{melt}, \qquad (1)$$

which is the sum of the homogeneous equilibrium $2FeO^{melt} + \tfrac{1}{2}O_2^{melt} = Fe_2O_3^{melt}$ and the heterogeneous equilibrium $O_2^{gas} = O_2^{melt}$. The equilibrium constant for Reaction 1 is defined by

$$K_1 \equiv \frac{[a^{melt}_{Fe_2O_3}]}{[a^{melt}_{FeO}]^2[f^{gas}_{O_2}]^{1/2}} \qquad (2)$$

where a denotes the activity and f denotes the fugacity of the subscripted species in the superscripted phase. Adopting a standard state consisting of the pure component at P and T makes the equilibrium constant K_1 a function of pressure and temperature alone. If the ferric and ferrous components mix ideally, then a plot of $\ln(X_{Fe_2O_3}/X^2_{FeO})$ (where ln refers to the natural logarithm and X_i denotes the mole fraction of the subscripted species i in the melt phase) against $\ln f_{O_2}$ should be linear, with a slope of one half. Deviations from such simple behavior will reflect nonideal mixing in ferric and/or ferrous components.

The response of the ferric/ferrous ratio of a silicate-melt phase to variations in temperature, oxygen fugacity, and composition has been investigated by several workers. Kennedy (1948) measured ferric and ferrous contents of a San Juan Mountains basalt equilibrated in air at temperatures between 800 °C and 1400 °C. Johnston (1964, 1965) carried out similar experiments on simple $Na_2O \cdot 2SiO_2$ glasses with less than 2 wt% iron. Johnston

0003–004X/88/1112–1267$02.00

(1964, 1965) found that a plot of $\ln(X_{Fe_2O_3}/X^2_{FeO})$ against $\ln f_{O_2}$ is linear with a slope of one half, consistent with the ideal-mixing model postulated above.

Densem and Turner (1938) demonstrated that composition plays a major role in determining ferric-ferrous equilibrium in silicate liquids. Paul and Douglas (1965) and Douglas et al. (1965) explored the effect of composition on ferric-ferrous equilibrium in binary alkali-silicate glasses with less than 0.5 wt% iron. They found that increased alkalis drove Equilibrium 1 to the right and that the magnitude of this effect increased in the series Li < Na < K. Fudali (1965) examined the response of ferric/ferrous ratio to oxygen fugacity for a variety of basaltic and andesitic rocks and confirmed that alkalis tend to increase the ferric iron content of the melt. Fudali (1965) noted that the slope of $\ln(X_{FeO_{1.5}}/X_{FeO})$ vs. $\ln f_{O_2}$ varies between 0.27 and 0.16 rather than the constant value of 0.25 expected if mixing were ideal. Carmichael and Nicholls (1967) observed that the oxidizing effect of alkalis is evident in a wide variety of natural samples. Thornber et al. (1980) doped a tholeiitic basalt with varying amounts of oxide components in air in order to examine this effect directly. They confirmed that addition of Na_2O, K_2O, and CaO increases the ferric/ferrous ratio of the melt substantially. Thornber et al. (1980) also noted that increases in Al_2O_3 and SiO_2 decrease this ratio slightly.

Numerous models have been advanced that qualitatively and quantitatively describe redox equilibria in quenched simple silicate melts (Toop and Samis, 1962a, 1962b; Douglas et al., 1965; Masson, 1965, 1968, 1972; Masson et al., 1970; Gaskell, 1977; Lauer, 1977; Lauer and Morris, 1977; Schreibner, 1986). Geologic applications of these models have been discussed by Hess (1980). The first comprehensive calibration of iron redox state in complex natural liquids as a function of oxygen fugacity, temperature, and bulk composition was given by Sack et al. (1980). Sack et al. (1980) performed a large number of Pt-loop experiments, primarily at oxygen fugacities close to those defined by the fayalite-magnetite-quartz (FMQ) assemblage. These experiments were combined with the superliquidus ferric-ferrous equilibrium experiments of Kennedy (1948), Shibata (1967), and Thornber et al. (1980) in order to quantitatively establish the dependence of ferric/ferrous ratio on oxygen fugacity, temperature, and the bulk composition of the melt. Regression of these data suggested that a model in which $\ln(X_{Fe_2O_3}/X^2_{FeO})$ is constrained to be linear in $\ln f_{O_2}$ results in a poor fit to the experimental data. Sack et al. (1980) found that a far better fit to observations could be obtained using a simple empirical expression of the form

$$\ln\left[\frac{X^{liq}_{Fe_2O_3}}{X^{liq}_{FeO}}\right] = a \ln f_{O_2} + \frac{b}{T} + c + \sum_i d_i X_i, \qquad (3)$$

where a, b, c, and d_i are regression coefficients and the sum is over the oxide components i. Kilinc et al. (1983) refined the compositional parameters d_i by supplementing the data of Sack et al. (1980) with 46 additional experiments, in air, on compositions ranging from nephelinite to rhyolite.

Mysen (1987) recently proposed a far more complicated model for estimation of ferric-ferrous equilibrium in silicate melts. This model differs from that proposed by Sack et al. (1980) in that it is based on a regression of inferred structural constituents in the melt. The data set employed in the regression of Mysen (1987) also includes a large portion (>50%) of simple three- and four-component compositions. With such an extreme range of compositions considered, it is not suprising that Mysen (1987) found that values for his regression coefficients were quite dependent on variations in the input data set.

It has been suggested (Mysen et al., 1984; Mysen et al., 1985a; Virgo and Mysen, 1985), on the basis of Mössbauer data, that the ferric ion undergoes a coordination change from fourfold to sixfold as $Fe^{3+}/(Fe^{2+} + Fe^{3+})$ is decreased below one half. Because fourfold and sixfold ferric iron are expected to play different structural roles in the melt, a progressive ferric coordination shift will almost certainly be accompanied by a change in the chemical potential of the ferric component and its derivatives. Such a coordination shift would, therefore, be likely to be expressed macroscopically in a change in the slope of $\ln(X_{Fe_2O_3}/X_{FeO})$ against $\ln f_{O_2}$. Existence of such a slope break would suggest that it is incorrect to apply the regression of Kilinc et al. (1983) at oxygen fugacities below FMQ.

Recent high-precision determinations of the ferric-ferrous distribution in mid-ocean ridge basalt (MORB) glasses (Christie et al., 1986) suggest that submarine basalts equilibrate under far more reducing conditions than had been previously believed. Using Reaction 3 with the regression coefficients of Kilinc et al. (1983), Christie et al. (1986) estimated quench oxygen fugacities up to 3 $\log_{10}$ units below the nickel–nickel oxide (NNO) oxygen buffer. These results suggest that MORBs are among the most reduced lavas on Earth. The most reduced experiments in the regression of Kilinc et al. (1983) were equilibrated at oxygen fugacities close to the fayalite-magnetite-quartz (FMQ) buffer (0.7 $\log_{10}$ units below NNO). The conclusions of Christie et al. (1986) are, therefore, based on an extrapolation of the regression of Kilinc et al. (1983) outside the range of experimental calibration.

In order to resolve these issues and to better define the stoichiometry of the iron oxidation reaction in silicate melts, we have performed ferric-ferrous equilibrium experiments on a limited number of compositions spanning a much larger and more complete range of temperature and f_{O_2} than had been examined previously.

Experimental technique

Starting materials consisted of ground rock powders that were first fused at 1400 °C in air, then broken into 1-g fragments. These fragments were welded onto 4-mm loops of 0.117-mm Pt_{90} Rh_{10} wire with an oxyacetylene torch. In each experiment, 10 loops, comprising 5 duplicate pairs, were suspended in the

hot spot of a vertical quench furnace. Oxygen fugacity was imposed by a furnace atmosphere consisting of a CO-CO_2 gas mixture (Deines et al., 1974). Gas-mixing ratios were controlled by calibrated floating-ball flow meters. Temperatures were measured by a Pt_{100} /Pt_{90} Rh_{10} thermocouple placed roughly 3 mm above the experiment cage. The thermocouple was isolated from the reducing furnace atmosphere by an alumina cement cap. Measurements of the melting point of 99.99% Au, both before and after the experiments, indicated temperatures of 1063.8 °C and 1063.1 °C, respectively. These values compare favorably with the accepted Au melting point of 1064.43 °C (IPTS, 1969). A 2° correction was added to adjust for measured temperature gradients inside the furnace.

Oxygen fugacities imposed by furnace gas mixtures were calibrated by measuring the temperature of iron-wüstite (Myers and Eugster, 1983), nickel–nickel oxide (Chou, 1978), and magnetite-hematite (Myers and Eugster, 1983) assemblages at the CO-CO_2 flow-rate combinations used in the experiments. These calibration experiments indicated oxygen fugacities that were 0.01 to 0.4 $\log_{10}$ units higher than those predicted by the Deines et al. (1974) calibration. Huebner (1975) noted a similar discrepancy between observed and predicted oxygen fugacities in CO-CO_2 gas mixtures. His results differ somewhat from ours, however, in that the discrepancy observed by Huebner (1975) is largely independent of mixing ratio, whereas we found that the difference between observed and predicted values was strongly correlated with the proportion of CO_2 in the gas. Our results suggest that the difference between the observed and predicted oxygen fugacities can be attributed to contamination of the CO_2 gas used in our experiments. This conclusion was confirmed by duplicate calibration experiments using 99.8 mol% pure, bone-dry–grade CO_2 gas instead of the commercial-grade CO_2 gas used in the ferric-ferrous equilibration experiments. The calibration experiments performed with the higher-purity gas indicated less than 0.1 $\log_{10}$ units discrepancy between f_{O_2} values predicted from Deines et al. (1974) and those indicated by the magnetite-hematite buffer curves of Myers and Eugster (1983) or Chou (1978). On the basis of these results, calibration corrections were applied to the individual experiments based on CO-CO_2 mixing ratio. Corrections ranged from +0.09 to +0.4 $\log_{10}$ units.

Duplicate runs of between 2 and 12 h duration indicated that experiments of longer than about 5 h showed continued alkali loss without significant change in the ferric/ferrous ratio. Shorter runs showed appreciable scatter in observed ferric/ferrous ratio. These results are consistent with those of Thornber et al. (1980) and Kilinc et al. (1983). Experiment durations between 5 and 8 h were considered an optimal compromise. Experiments were quenched by dropping into cold distilled H_2O that had been previously boiled. Though complete equilibration requires 5 to 8 h, experiments indicate that the ferric/ferrous ratio can be substantially altered in as little as 30 s. For this reason, our apparatus was designed so that the quench could be carried out under the reducing-furnace atmosphere. Experiments were performed at 1360 °C and 1460 °C at oxygen fugacities between air and 5.2 $\log_{10}$ units below NNO at 1 to 3 $\log_{10}$ unit invervals. For the experiments that were performed at higher oxygen fugacities, no effort was made to presaturate the loops in iron. Iron loss in these runs was often found to be quite significant (20–30% of the amount present). Electron-microprobe traverses of quench glass beads from these experiments revealed no detectable gradient in total iron concentration. On the basis of this evidence, we assume that equilibrium saturation was closely approached during these experiments. For experiments at very low f_{O_2} and in compositions with low initial total iron content, loops were used that had been previously saturated in an iron-rich melt and cleaned in 50% HF solution.

All experiments were examined under a polarizing microscope to verify the absence of a crystalline phase. Run products were analyzed for major and minor elements on an eight-channel ARL-SEMQ electron microprobe using an accelerating potential of 15 kV, a sample current of 0.03 μA on brass, a spot size of roughly 5 μm, and a 10-s integration time. Analyses made while scanning the beam across the sample or using a defocused beam yielded no detectable difference in alkali content, but noticeably decreased the analytical precision. For this reason, neither of these techniques was employed. Data reduction was carried out with the empirical correction scheme of Bence and Albee (1968) using basaltic glass (USNM 113498) (Si, Al, Ti, Fe, and Mg), labradorite (Na and Ca), orthoclase (K), chlor-apatite (P), chromite (Cr), and V_2O_3 (V) as standards. For each glass sample, 22–24 points were analyzed. The means of analyses for each experiment are listed in Table 1. Standard deviations of major-element analyses are between 0.8 and 8.0% relative. Ferrous iron contents were determined using wet-chemical techniques. Ferric iron is calculated from the difference between total iron and iron in the ferrous state [$Fe_2O_3 = 1.1113(FeO^* - FeO)$ where FeO* is total iron as FeO].

Two series of experiments were performed. In the first series, four compositions were equilibrated at 1360 °C and 1460 °C at 1 to 3 $\log_{10}$ unit intervals between air and 5.2 log units below NNO. These experiments allow us to establish the response of iron oxidation state to variations in oxygen fugacity, with temperature and all components except FeO and Fe_2O_3 held constant. In the second series, a single composition (JDFD2) was equilibrated at roughly 50 °C intervals between 1299 °C and 1636 °C at approximately 0.2 $\log_{10}$ units below FMQ (Table 1; samples 103 and B111–B120) in order to determine the temperature dependence of the iron oxidation reaction at nearly constant ferric/ferrous ratio.

Results and discussion

Figures 1a to 1d are plots of $\ln(X_{Fe_2O_3}/X^2_{FeO})$ against $\ln f_{O_2}$ at approximately 1360 °C for four of the compositions studied. The short lines at the upper right side of these plots have a slope of 0.5 and are provided in order to illustrate the slope expected if FeO-Fe_2O_3 mixing were ideal. The observed slopes are closer to 0.3 and are clearly inconsistent with ideal mixing of these components. Similar results were obtained in a series of experiments performed on these same compositions at 1460 °C. It is, in fact, quite remarkable that both the slope and curvature of the plot of $\ln(X_{Fe_2O_3}/X^2_{FeO})$ vs. $\ln f_{O_2}$ seem to be largely independent of composition over the range considered.

Our data are consistent with earlier results (Sack et al., 1980) that suggest that $\ln(X_{Fe_2O_3}/X_{FeO})$, rather than $\ln(X_{Fe_2O_3}/X^2_{FeO})$, is linear in $\ln f_{O_2}$. Regressions in which the dependent variable is $\ln(X_{Fe_2O_3}/X^2_{FeO}$ show pronounced U-shaped structure in a plot of residuals against predicted values. Similar plots for regressions in which $\ln(X_{Fe_2O_3}/X_{FeO})$ is the dependent variable show no such structure. Linear best-fit lines for $\ln(X_{Fe_2O_3}/X_{FeO})$ vs. $\ln f_{O_2}$ plots for the compositions considered have an average slope of 0.2071 ± 0.0072 (2σ), which is somewhat lower than the value 0.2185 ± 0.0044 obtained by Kilinc et al. (1983). The slopes suggested by the plots of 780-U-105 composition

TABLE 1. Compositions (in wt%) and conditions for individual experiments

	71	74	79	83	86	89	91	100	101	102	103
Composition	JDFD2	780-U-105	JDFD2	JDFD2	780-U-105	JDFD2	20424	COL-11	20424	780-U-105	JDFD2
T (°C)	1461	1461	1459	1459	1459	1459	1459	1459	1459	1459	1459
$\log_{10} f_{O_2}$	−7.17	−7.17	−8.21	−8.21	−8.21	−9.21	−9.21	−6.15	−6.15	−6.15	−6.15
SiO_2	51.36	42.12	52.57	51.76	42.78	52.03	42.75	56.81	41.11	41.84	51.28
TiO_2	1.90	6.06	1.94	1.95	6.19	1.95	3.20	0.74	3.07	5.91	1.91
Al_2O_3	14.02	10.58	14.23	14.16	10.65	14.23	14.77	17.01	14.36	10.48	13.99
Fe_2O_3	1.09	1.93	0.76	0.78	0.98	0.58	0.70	0.86	2.06	2.88	2.04
Cr_2O_3	0.02	0.02	0.02	0.02	0.02	0.02	0.02	0.03	0.02	0.01	0.02
FeO	10.34	11.66	8.79	10.00	11.97	8.81	9.50	5.09	9.31	10.37	9.47
MnO	0.25	0.31	0.25	0.24	0.32	0.25	0.43	0.15	0.41	0.32	0.25
MgO	6.93	7.33	7.03	7.06	7.40	7.04	6.40	6.26	6.30	7.05	6.93
CaO	10.50	15.51	10.70	10.53	15.90	10.77	18.79	7.28	18.02	15.48	10.35
Na_2O	2.29	0.62	2.38	2.26	0.70	2.06	0.63	4.12	1.42	1.30	2.77
K_2O	0.72	1.53	1.08	0.84	0.52	1.64	0.33	1.80	1.32	1.87	0.66
P_2O_5	0.20	0.09	0.13	0.15	0.10	0.14	0.21	0.15	0.42	0.19	0.16
V_2O_3	0.06	0.12	0.06	0.05	0.12	0.06	0.08	0.02	0.08	0.12	0.05
Total	99.68	97.88*	99.94	100.61	97.65*	99.58	97.06*	100.14	97.90*	97.82*	99.88

	107	121	125	129	130	131	132	137	139	141	142
Composition	K-1919	20424	20424	JDFD2	COL-11	20424	780-U-105	K-1919	JDFD2	20424	780-U-105
T (°C)	1459	1458	1458	1455	1455	1455	1455	1455	1362	1362	1362
$\log_{10} f_{O_2}$	−6.15	−10.23	−10.23	−2.42	−2.42	−2.42	−2.42	−2.42	−7.93	−7.93	−7.93
SiO_2	49.97	43.62	43.98	49.08	56.89	39.41	39.77	49.22	51.11	40.34	41.12
TiO_2	2.86	3.24	3.21	1.81	0.74	2.84	5.84	2.75	1.95	3.01	6.11
Al_2O_3	14.04	15.39	14.71	13.65	16.91	14.21	10.06	13.82	14.09	13.90	10.60
Fe_2O_3	1.58	0.52	0.68	7.43	2.89	8.23	9.21	5.80	1.10	1.12	1.23
Cr_2O_3	0.04	0.02	0.14	0.02	0.04	0.03	0.02	0.04	0.04	0.04	0.02
FeO	9.09	8.44	8.46	6.93	3.75	3.98	5.19	5.36	9.68	9.97	11.56
MnO	0.19	0.43	0.40	0.22	0.13	0.17	0.13	0.09	0.11	0.19	0.14
MgO	7.17	6.49	6.59	6.61	6.39	5.87	6.90	6.91	6.94	6.11	7.17
CaO	10.89	18.86	19.14	10.27	7.31	17.29	14.89	10.82	10.53	17.70	15.45
Na_2O	2.74	0.62	0.53	2.95	3.87	3.67	2.29	2.83	3.11	2.50	1.60
K_2O	1.20	0.34	0.29	0.70	1.44	2.80	3.83	1.55	0.94	2.49	3.12
P_2O_5	0.25	0.08	0.07	0.29	0.20	0.59	0.22	0.37	0.35	1.27	0.66
V_2O_3	0.06	0.09	0.12	0.06	0.03	0.07	0.11	0.05	0.06	0.08	0.11
Total	100.08	98.14*	98.32*	100.02	100.59	99.16*	98.46*	99.61	100.01	98.72*	98.89*

	147	151	155	159	160	161	167	169	171	172	174
Composition	KIL-2	20424	20424	JDFD2	COL-11	20424	KIL-2	JDFD2	20424	780-U-105	COL-11
T (°C)	1362	1361	1361	1361	1361	1361	1361	1364	1364	1364	1364
$\log_{10} f_{O_2}$	−7.93	−9.97	−9.97	−2.74	−2.74	−2.74	−2.74	−5.86	−5.86	−5.86	−5.86
SiO_2	50.06	42.08	42.30	50.22	56.77	38.67	50.45	50.65	39.60	39.89	57.17
TiO_2	3.24	3.03	3.16	1.91	0.74	2.88	3.21	1.93	2.91	5.84	0.73
Al_2O_3	13.85	14.85	14.41	13.77	16.91	13.35	13.13	13.50	13.58	9.99	16.89
Fe_2O_3	1.17	0.79	0.67	7.18	3.65	8.27	6.99	1.96	3.28	3.51	1.01
Cr_2O_3	0.04	0.04	0.13	0.02	0.03	0.03	0.05	0.04	0.04	0.04	0.10
FeO	10.37	10.10	9.62	5.34	3.22	3.89	4.84	9.38	7.83	9.62	4.95
MnO	0.08	0.19	0.42	0.13	0.06	0.18	0.19	0.22	0.39	0.29	0.13
MgO	6.29	6.25	6.37	6.74	6.27	5.83	6.28	6.79	6.08	7.07	6.26
CaO	9.79	18.62	18.58	10.39	7.34	17.12	9.85	10.57	17.54	15.13	7.29
Na_2O	3.03	1.12	1.05	2.81	3.84	4.15	2.54	2.94	3.15	2.05	4.04
K_2O	1.29	0.98	0.91	0.53	1.24	3.22	0.91	0.69	3.00	4.38	1.45
P_2O_5	0.38	0.50	0.45	0.46	0.29	0.89	0.49	0.35	1.09	0.59	0.23
V_2O_3	0.06	0.07	0.12	0.05	0.02	0.07	0.07	0.07	0.07	0.12	0.04
Total	99.65	98.62*	98.19*	99.55	100.38	98.55*	99.00	99.09	98.56*	98.52*	100.29

	177	199	202	205	208	209	210	211	212	218
Composition	KIL-2	JDFD2	780-U-105	20424	KIL-2	JDFD2	COL-11	780-U-105	20424	KIL-2
T (°C)	1364	1366	1366	1366	1366	1360	1360	1360	1360	1360
$\log_{10} f_{O_2}$	−5.86	−8.91	−8.91	−8.91	−8.91	−0.68	−0.68	−0.68	−0.68	−0.68
SiO_2	50.77	51.93	41.47	41.92	51.41	50.55	56.81	40.33	38.85	50.66
TiO_2	3.23	1.97	6.06	3.19	3.29	1.89	0.71	5.87	2.91	3.21
Al_2O_3	13.56	14.41	10.65	14.38	13.64	13.69	16.71	10.05	13.46	13.53
Fe_2O_3	2.17	0.69	1.03	1.05	0.57	9.77	5.12	12.59	10.69	9.33
Cr_2O_3	0.10	0.03	0.02	0.14	0.10	0.00	0.00	0.01	0.02	0.01
FeO	8.78	10.08	13.68	10.40	10.49	3.10	1.82	2.51	1.97	3.06
MnO	0.17	0.10	0.13	0.41	0.19	0.22	0.13	0.28	0.37	0.18
MgO	6.29	6.88	7.15	6.32	6.46	6.71	6.20	6.91	5.80	6.30
CaO	9.60	10.87	15.72	18.37	9.86	10.40	7.43	15.09	17.53	9.72
Na_2O	3.05	1.72	0.55	0.47	2.09	2.58	3.63	1.88	3.52	2.37
K_2O	1.39	0.68	1.44	0.54	0.83	0.43	1.10	2.77	1.90	0.67
P_2O_5	0.50	0.56	0.55	1.10	0.43	0.21	0.11	0.09	0.51	0.15
V_2O_3	0.11	0.05	0.12	0.12	0.11	0.06	0.03	0.12	0.07	0.07
Total	99.72	99.97	98.57*	98.41*	99.47	99.61	99.80	98.50*	97.60*	99.26

TABLE 1.—*Continued*

	229	230	231	236	238	B27	B34	B44	B54	B64
Composition	JDFD2	COL-11	20424	780-U-105	KIL-2	JDFD2	JDFD2	JDFD2	JDFD2	JDFD2
T (°C)	1458	1458	1458	1458	1458	1437	1388	1485	1535	1584
$\log_{10} f_{O_2}$	−0.68	−0.68	−0.68	−0.68	−0.68	−0.68	−0.68	−0.68	−0.68	−0.68
SiO_2	50.93	57.27	40.78	41.14	51.15	50.46	50.64	50.61	51.09	51.00
TiO_2	1.91	0.74	3.01	5.93	3.28	1.88	1.89	1.90	1.89	1.92
Al_2O_3	13.67	16.76	13.49	10.25	13.77	13.87	13.93	14.03	13.94	13.96
Fe_2O_3	8.69	4.51	10.02	11.24	8.29	9.46	9.91	8.94	8.38	7.60
Cr_2O_3	0.01	0.01	0.03	0.02	0.01	0.02	0.02	0.02	0.02	0.01
FeO	4.14	2.45	3.00	3.65	3.81	3.49	2.92	3.96	4.46	5.12
MnO	0.22	0.13	0.38	0.27	0.17	0.17	0.17	0.17	0.17	0.17
MgO	6.96	6.32	6.04	7.12	6.14	6.84	6.76	6.66	6.77	6.86
CaO	10.40	7.42	17.97	15.40	9.79	10.65	10.66	10.61	10.67	10.69
Na_2O	2.47	3.60	2.68	1.39	2.29	2.68	2.66	2.43	2.43	2.32
K_2O	0.36	1.02	0.97	1.70	0.61	0.19	0.19	0.17	0.17	0.16
P_2O_5	0.09	0.10	0.09	0.01	0.04	0.10	0.16	0.05	0.04	0.02
V_2O_3	0.05	0.02	0.08	0.11	0.07	0.06	0.06	0.06	0.05	0.05
Total	99.90	100.35	98.54*	98.23*	99.42	99.87	99.97	100.03+	99.68+	100.33+

	B73	B76	B79	B82	B105	B111	B112	B113	B118	B120
Composition	JDFD2	JDFD2	JDFD2	JDFD2	JDFD2	JDFD2	JDFD2	JDFD2	JDFD2	JDFD2
T (°C)	1635	1342	1296	1249	1636	1363	1363	1299	1544	1632
$\log_{10} f_{O_2}$	−0.68	−2.89	−3.07	−3.26	−6.29	−6.81	−6.81	−7.38	−5.42	−4.74
SiO_2	51.22	51.24	50.90	50.38	52.50	52.39	52.35	51.42	52.02	52.02
TiO_2	1.93	1.91	1.91	1.93	2.02	1.96	1.98	2.00	1.99	1.98
Al_2O_3	13.91	13.81	13.85	13.70	14.52	13.96	14.25	14.12	14.30	14.28
Fe_2O_3	7.02	8.21	8.46	9.00	1.46	2.07	1.96	2.19	2.94	2.75
Cr_2O_3	0.01	0.02	0.02	0.02	0.03	0.03	0.02	0.02	0.04	0.03
FeO	5.58	4.55	4.46	3.91	10.26	9.84	9.54	9.18	9.65	10.01
MnO	0.17	0.17	0.17	0.17	0.21	0.22	0.21	0.22	0.21	0.23
MgO	6.80	6.78	6.82	6.93	7.24	7.06	7.11	7.19	7.16	7.21
CaO	10.66	10.52	10.61	10.54	11.53	11.17	11.31	11.40	11.37	11.41
Na_2O	2.22	2.67	2.69	2.70	0.56	2.38	2.33	2.65	1.22	0.85
K_2O	0.15	0.21	0.20	0.20	0.14	0.20	0.17	0.21	0.14	0.12
P_2O_5	0.01	0.20	0.24	0.21	0.05	0.17	0.21	0.24	0.05	0.03
V_2O_3	0.04	0.06	0.05	0.05	0.09	0.08	0.07	0.08	0.08	0.09
Total	99.72	100.35	100.38	99.74	100.61	101.53	101.51	100.92	101.17	101.01

* Totals for 780-U-105 and 20424 do not reflect contributions of SrO, BaO, and other minor elements that are significant in these compositions.

are slightly higher than those suggested by the other compositions, but this difference is within the analytical uncertainty.

The fact that the behavior observed in Figures 1a–1d is largely independent of bulk melt composition suggests that this effect must reside primarily in interactions between the ferric and ferrous cations. This is consistent with a suggestion made by Virgo and Mysen (1985) that clusters with Fe_3O_4 stoichiometry may be present in the melt at intermediate oxygen fugacities. An ideal-mixing model involving partial or complete association of ferric and ferrous components to a Fe_3O_4 cluster produces curves with the sort of overall slope observed in the experiments, but the shapes of the curves so produced are significantly convex upward. This is not in accord with observations.

There is no indication of a slope break in any of the plots in Figure 1, suggesting that there is probably no

TABLE 2. Coefficients for estimation of redox equilibria

Coefficient	Value	Standard error	Units
ΔH	−95.93	6.39	kJ
ΔS	−46.05	3.55	J/K
$\Delta W_{Al_2O_3}$	49.04	15.53	kJ
ΔW_{CaO}	−48.87	6.71	kJ
ΔW_{Na_2O}	−106.04	20.64	kJ
ΔW_{K_2O}	−110.46	19.52	kJ
R^2	0.95		
Standard error	0.30		

$$\ln\left[\frac{X^{liq}_{FeO_{1.464}}}{X^{liq}_{FeO}}\right] = 0.232 \ln f_{O_2} - \frac{\Delta H_4}{RT} + \frac{\Delta S_4}{R} - \frac{1}{RT}\sum_i \Delta W_i X_i$$

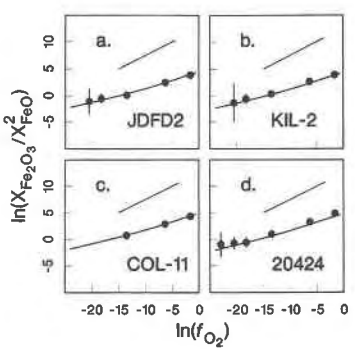

Fig. 1. Plot of $\ln(X_{Fe_2O_3}/X^2_{FeO})$ against $\ln f_{O_2}$ for four compositions at 1360 °C. Error bars represent estimated 2σ analytical error. Where error bars not present, error is smaller than data marker. The curves in these plots are predicted using the model in Table 2. The short lines at the upper right of the figures represent the slope expected if FeO-Fe_2O_3 mixing were ideal.

abrupt change in melt properties over the range of oxygen fugacities examined. This does not rule out a possible ferric ion coordination change within this range. A gradual coordination shift, distributed over a somewhat larger range of $Fe^{3+}/(Fe^{2+} + Fe^{3+})$ could conceivably contribute to the unusual behavior displayed in Figure 1.

A far simpler explanation becomes evident if one considers ferric-ferrous clusters of more arbitrary stoichiometry. It was found that the data can be remarkably well represented by a model based on simple mixing between FeO and a completely associated $FeO_{1.464\pm0.003}$ (approximately $FeO \cdot 6Fe_2O_3$) component. In terms of these components, the iron oxidation reaction takes the form

$$FeO + 0.232O_2 = FeO_{1.464}. \quad (4)$$

Analyses are easily recast in terms of this unusual component by first converting to mole fraction using $FeO_{1.5}$ (molecular weight 79.849) rather than Fe_2O_3 to represent the ferric component. $X_{FeO_{1.464}}$ and X_{FeO} can then be estimated by the relations

$$X_{FeO_{1.464}} = 1.0776X_{FeO_{1.5}} \quad (5)$$

$$X_{FeO} = X_{FeO} - 0.0776X_{FeO_{1.5}}. \quad (6)$$

A complete symmetric Margules formulation for Reaction 4 takes the form

$$\ln(K_4) = -\frac{\Delta H_4}{RT} + \frac{\Delta S_4}{R} - \frac{1}{RT}\int_{T_r}^{T} \Delta C_{P_4}\, dT + \frac{1}{R}\int_{T_r}^{T} \frac{\Delta C_{P_4}}{T}\, dT - \frac{1}{RT}\sum_i (W_{i,FeO_{1.464}} - W_{i,FeO})X_i, \quad (7)$$

where ΔH_4, ΔS_4, and ΔC_{P_4} are the enthalpy, entropy, and heat-capacity change of Reaction 1, respectively, R is the universal gas constant, T is in kelvins and T_r is the reference temperature in kelvins. In this formulation, the deviation from ideality resides in the Margules mixing terms ($W_{i,j}$ where $W_{i,j} = W_{j,i}$ and $W_{i,i} = 0$). $W_{FeO,FeO_{1.464}}$ is set equal to zero. The distribution coefficient (K_{D4}) is defined as

$$K_{D4} \equiv \frac{[X^{melt}_{Fe_{1.464}}]}{[X^{melt}_{FeO}][f_{O_2}]^{0.232}}. \quad (8)$$

Estimates can be made of the magnitudes of ΔH_4 and ΔC_{P_4} using data from Stebbins et al. (1984) and Chase et al. (1985). These estimates suggest that, between 1230 °C and 1630 °C, the change in $\ln K_4$ due to the ΔC_{P_4} terms is probably less than 5% of the contribution due to the ΔH_4 term. This corresponds to a contribution due to ΔC_{P_4} of less than 0.25 ln units, significantly beneath the data resolution. By adopting a reference temperature of 1673 K, a point that is interior to the data, we can justifiably neglect the ΔC_{P_4} terms, considerably simplifying Equation 7.

The solid curves in Figures 1a to 1d are calculated from a model of the form

$$\ln\left[\frac{X^{liq}_{FeO_{1.464}}}{X^{liq}_{FeO}}\right] = 0.232 \ln f_{O_2} - \frac{\Delta H_4}{RT} + \frac{\Delta S_4}{R} - \frac{1}{RT}\Sigma_i \Delta W_i X_i \quad (9)$$

(where $\Delta W_i \equiv W_{i,FeO_{1.464}} - W_{i,FeO}$) with coefficients from Table 2. These coefficients were estimated by stepwise linear regression of experimental results from this study, along with the database of Kilinc et al. (1983) and Sack et al. (1980). The most highly reduced experiments ($\log_{10} f_{O_2}$ less than −9.5) were omitted from this regression to prevent these less-certain data from exerting undue influence on the regression. Plots such as those in Figures 1a–1d verify that this regression reproduces even the more reduced data well within their analytical uncertainty. One of the data points from the Kilinc et al. (1983) data set on the 20424 composition is a serious outlier in both regressions and is clearly inconsistent with results from this study on the same composition under nearly identical conditions. Omission of this point substantially improved the precision of the regression. Equation 9 reproduces the experimental data with a standard error of 0.3 ln units. The estimated value for ΔH_4 is comparable to experimentally determined ΔH values for the FMQ solid buffer (−86 kJ·mol^{-1} at 1723 K, recast in terms of an equivalent number of exchanged oxygens, O'Neil, 1987) but somewhat more negative than that measured for NNO (−54 kJ·mol^{-1} at 1723 K, similarly recast, Holms et al., 1986).

The positive sign of the $\Delta W_{Al_2O_3}$ term is consistent with the interpretation that tetrahedrally coordinated trivalent iron and aluminum compete for charge-balancing alkalis in peraluminous melts (Dickenson and Hess, 1981), thus leading to a positive enthalpy of mixing between these species. The negative signs of the ΔW terms for CaO, Na_2O, and K_2O are also in accord with the interpretation that these cations play a charge-balancing role in the melt. The relative magnitudes of the CaO, Na_2O, and K_2O terms are in agreement with the results of past workers (Paul and Douglas, 1965; Douglas et al., 1965; Thornber et al., 1980; Sack et al., 1980; Kilinc et al., 1983).

It should be emphasized that the postulated $FeO_{1.464}$ component may not represent a discrete species existing in the melt. Rather, this unusual stoichiometry likely reflects the most probable of a distribution of configurations, almost certainly involving other cations in the melt. Nevertheless, regressions of various subsets of the total database result in nearly identical estimates of the stoichiometry of this component, suggesting that this property must reflect some fundamental aspect of the structure of natural silicate melts. Our macroscopic data do not resolve this issue, but do provide hints of potentially profitable lines of future inquiry. For now, the primary advantage of the formulation represented by Reaction 4

is that it allows a simple ferric/ferrous mixing model to be applied to natural silicate compositions. By casting compositions in terms of FeO and $FeO_{1.464}$ components, ferric-ferrous mixing terms are avoided, resulting in simpler and more mathematically stable thermodynamic formulations (Ghiorso, 1985).

As a direct comparison of the regression presented in this study with the best previously available calibration (Kilinc et al., 1983), we rearranged Equations 9 and 3 to back-calculate $\ln(Fe_2O_3/FeO)$, $\ln f_{O_2}$, and T for each of the experiments in the entire data set. The mean of the residuals (observed − calculated) for the Kilinc et al. (1983) regression for $\ln(Fe_2O_3/FeO)$ is −0.020 ln units with a standard deviation of 0.301. Back-calculation of $\ln(Fe_2O_3/FeO)$ using the data in Table 2 results in residuals with a mean of 0.004 and a standard deviation of 0.291 ln units. It is encouraging that Equation 9 reproduces $\ln(Fe_2O_3/FeO)$ better than the regression of Kilinc et al. (1983) despite the fact that it contains one fewer fit parameters and was regressed on a different dependent variable. Application of the Kilinc et al. regression to back-calculate $\ln f_{O_2}$ results in a residual mean of 0.039 ln units and a standard deviation of 0.599. Our results lead to a residual mean and standard deviation of −0.015 and 0.597 ln units, respectively. The mean and standard deviation of the residuals for back-calculation of T are −4.1 °C and 62.8 °C, respectively, for the Kilinc et al. (1983) regression and −0.06 °C and 69.1 °C, respectively, for the regression presented in this study.

The results presented in this study confirm that Equation 9 remains valid to oxygen fugacities as low as those defined by the iron-wüstite assemblage. Application of the coefficients in Table 2 to the ferric-ferrous determinations of Christie et al. (1986) yields estimated values of $\ln f_{O_2}$ between 0.09 and 0.24 $\log_{10}$ units lower than those predicted using the coefficients of Kilinc et al. (1983). This difference is quite small and does not challenge the validity of the conclusions reached by Christie et al. (1986).

Conclusions

We have demonstrated that the iron oxidation reaction in silicate melts is well represented by a formulation involving oxidation of FeO to a completely associated $FeO_{1.464}$ component. Thermodynamic parameters are presented that describe the iron oxidation reaction in terms of these components. This regression is valid to oxygen fugacities as low as those defined by the iron-wüstite assemblage. The model presented in this study is a thermodynamically based calibration of the iron oxidation reaction in basic silicate melts and represents the most precise relation between ferric/ferrous ratio, oxygen fugacity, temperature, and bulk composition available.

Acknowledgments

This text has benefited from discussions with D. Snyder and careful reviews by J. Nicholls and an anonymous reviewer. M. Ghiorso suggested a clever method for determining the stoichiometry of ideally mixing components and provided valuable advice regarding numerical methods. This work was supported, in part, by National Science Foundation grants EAR 85-00813 and OCE 86-13262 and, in part, by the Department of Energy contract DEAC03-76SF00098.

References cited

Bence, A.E., and Albee, A.L. (1968) Empirical correction factors for the electron microanalysis of silicates and oxides. Journal of Geology, 76, 382–403.

Bottinga, Y., Weill, D.F., and Richet, P. (1982) Density calculations for silicate liquids. I. Revised method for aluminosilicate compositions. Geochimica et Cosmochimica Acta, 46, 909–919.

Bottinga, Y., Richet, P., and Weill, D.F. (1983) Calculation of the density and thermal expansion coefficient of silicate liquids. Bulletin de Minéralogie, 106, 129–138.

Carmichael, I.S.E., and Nicholls, J. (1967) Iron-titanium oxides and oxygen fugacities in volcanic rocks. Journal of Geophysical Research, 72, 18, 4665–4686.

Chase, M.W., Jr., Davies, C.A., Downey, J.R., Jr., Frurip, D.J., McDonald, R.A., and Syverud, A.N. (1985) JANAF thermochemical tables (3rd edition). Journal of Physical and Chemical Reference Data, 14, 1856 p.

Chou, I.M. (1978) Calibration of oxygen buffers at elevated P and T using the hydrogen fugacity sensor. American Mineralogist, 63, 690–703.

Christie, D.M., Carmichael, I.S.E., and Langmuir, C.H. (1986) Oxidation states of mid-ocean ridge basalt glasses. Earth and Planetary Science Letters, 79, 397–411.

Cukierman, M., and Uhlmann, D.R. (1974) Effect of iron oxidation state on viscosity, lunar composition 1555. Journal of Geophysical Research, 79, 1594–1598.

Deines, P., Nafziger, R.H., Ulmer, G.C., and Woermann, E. (1974) Temperature-oxygen fugacity tables for selected gas mixtures in the system C-H-O at one atmosphere total pressure. Bulletin of the Earth and Mineral Sciences Experiment Station, 88, 129 p.

Densem, N.E., and Turner, W.E.S. (1938) The equilibrium between ferrous and ferric oxides in glasses. Journal of the Society of Glass Technology, 22, 372–389.

Dickenson, M.P., and Hess, P.C. (1981) Redox equilibria and the structural role of iron in alumino-silicate melts. Contributions to Mineralogy and Petrology, 78, 352–357.

Douglas, R.W., Nath, P., and Paul, A. (1965) Oxygen ion activity and its influence on the redox equilibrium in glasses. Physics and Chemistry of Glasses, 6, 216–223.

Drickamer, H.G., Lewis, G.K., Jr., and Fung, S.C. (1969) The oxidation state of iron at high pressure. Science, 163, 885–890.

Fudali, R.F. (1965) Oxygen fugacities of basaltic and andesitic magmas. Geochimica et Cosmochimica Acta, 29, 1063–1075.

Gaskell, D.R. (1977) Activities and free energies of mixing in binary silicate melts. Metallurgical Transactions B, 8B, 131–145.

Ghiorso, M.S. (1985) Chemical mass transfer in magmatic processes: I. Thermodynamic relations and numerical algorithms. Contributions to Mineralogy and Petrology, 90, 107–120.

Henderson, R.G., Hudson, R.G., Ward, R.G., and Derge, G. (1961) Density of liquid iron silicates. Transactions of the Metallurgical Society of AIME, 221, 807–811.

Hess, P.C. (1980) Polymerization model of silicate melts. In R.B. Hargraves, Ed., Physics of magmatic processes, p. 289–306. Princeton University Press, Princeton, N.J.

Holms, R.D., O'Neil, H.St.C., and Arculus, R.J. (1986) Standard Gibbs free energy of formation for Cu_2O, NiO, CoO, and Fe_xO: High resolution electrochemical measurements using zirconia solid electrolytes from 900–1400 K. Geochimica et Cosmochimica Acta, 50, 2439–2452.

Huebner, J.S. (1975) Oxygen fugacity values of furnace gas mixtures. American Mineralogist, 60, 815–823.

IPTS. (1969) The International Practical Temperature Scale of 1968. Meteorologia, 5, 35–44.

Johnston, W.D. (1964) Oxidation-reduction equilibria in iron-containing glass. Journal of the American Ceramic Society, 47, 198–201.

——— (1965) Oxidation-reduction equilibria in molten Na_2O-SiO_2 glass. Journal of the American Ceramic Society, 48, 184–190.

Kennedy, G.C. (1948) Equilibrium between volatiles and iron oxides in igneous rocks. American Journal of Science, 246, 529–549.

Kilinc, A., Carmichael, I.S.E., Rivers, M.L., and Sack, R.O. (1983) The ferric-ferrous ratio of natural silicate liquids equilibrated in air. Contributions to Mineralogy and Petrology, 83, 136–140.

Lange, R., and Carmichael, I.S.E. (1987) Densities of Na_2O-K_2O-CaO-MgO-FeO-Fe_2O_3-Al_2O_3-TiO_2-SiO_2 liquids: New measurements and derived partial molar properties. Geochimica et Cosmochimica Acta, 51, 2931–2946.

Lauer, H.V., Jr. (1977) Effect of glass composition on major element redox equilibria: Fe^{2+}-Fe^{3+}. Physics and Chemistry of Glasses, 18, 49–52.

Lauer, H.V., Jr., and Morris, R.V. (1977) Redox equilibria of multivalent ions in silicate glasses. Journal of the American Ceramic Society, 60, 443–451.

Masson, C.R. (1965) An approach to the problem of ionic distribution in liquid silicates. Proceedings of the Royal Society of London, A287, 201–221.

——— (1968) Ionic equilibria in liquid silicates. Journal of the American Ceramic Society, 51, 134–143.

——— (1972) Thermodynamics and constitution of silicate slags. Journal of the Iron and Steel Institute, 210, 89–96.

Masson, C.R., Smith, I.B., and Whiteway, S.G. (1970) Activities and ionic distributions in liquid silicates: Application of polymer theory. Canadian Journal of Chemistry, 48, 1456–1464.

Mo, X., Carmichael, I.S.E., Rivers, M., and Stebbins, J. (1982) The partial molar volume of Fe_2O_3 in multicomponent silicate liquids and the pressure dependence of oxygen fugacity in magmas. Mineralogical Magazine, 45, 237–245.

Myers, J., and Eugster, H.P. (1983) The system Fe-Si-O: Oxygen buffer calibrations to 1500 K. Contributions to Mineralogy and Petrology, 82, 75–90.

Mysen, B.O. (1987) Magmatic silicate melts: Relations between bulk composition, structure, and properties. In B.O. Mysen, Ed., Magmatic processes: Physiochemical principles, Geochemical Society Special Publication no. 1, p. 375–399. Geochemical Society, University Park, Pennsylvania.

Mysen, B.O., Virgo, D., and Seifert, F.A. (1984) Redox equilibria of iron in alkaline earth silicate melts: Relationships between melt structure, oxygen fugacity, temperature, and properties of iron-bearing silicate liquids. American Mineralogist, 69, 834–847.

Mysen, B.O., Virgo, D., Neuman, E.R., and Seifert, F.A. (1985a) Redox equilibria and the structural states of ferric and ferrous iron in melts in the system CaO-MgO-Al_2O_3-SiO_2-Fe-O: Relationships between redox equilibria, melt structure, and liquidus phase equilibria. American Mineralogist, 70, 317–331.

Mysen, B.O., Virgo, D., Scarfe, C.M., and Cronin, D.J. (1985b) Viscosity and structure of iron- and aluminum-bearing calcium silicate melts at 1 atm. American Mineralogist, 70, 487–498.

O'Neill, H.St.C. (1987) Quartz-fayalite-iron and quartz-fayalite-magnetite equilibria and the free energy of formation of fayalite (Fe_2SiO_4) and magnetite (Fe_3O_4). American Mineralogist, 72, 67–75.

Paul, A., and Douglas, R.W. (1965) Ferrous-ferric equilibrium in binary alkali silicate glasses. Physics and Chemistry of Glasses, 6, 207–211.

Sack, R.O., Carmichael, I.S.E., Rivers, M., and Ghiorso, M.S. (1980) Ferric-ferrous equilibria in natural silicate liquids at 1 bar. Contributions to Mineralogy and Petrology, 75, 369–376.

Schreibner, H.D. (1986) Redox processes in glass-forming melts. Journal of Non-Crystalline Solids, 84, 129–141.

Shibata, K. (1967) The oxygen partial pressure of the magma from Migara volcano, O-shima, Japan. Bulletin of the Chemical Society of Japan, 40, 830–834.

Stebbins, J.F., Carmichael, I.S.E., and Moret, L.K. (1984) Heat capacities and entropies of silicate liquids and glasses. Contributions to Mineralogy and Petrology, 86, 131–148.

Thornber, C.R., Roeder, P.L., and Foster, J.R. (1980) The effect of composition on the ferric-ferrous ratio in basaltic liquids at atmospheric pressure. Geochimica et Cosmochimica Acta, 44, 525–532.

Toop, G.W., and Samis, C.S. (1962a) Activities of ions in silicate melts. Transactions of the Metallurgical Society of AIME, 224, 878–887.

——— (1962b) Some new ionic concepts of silicate slags. Canadian Metallurgical Quarterly, 1, 129–152.

Virgo, D., and Mysen, B.O. (1985) The structural state of iron in oxidized vs. reduced glasses at 1 atm: A ^{57}Fe Mössbauer study. Physics and Chemistry of Minerals, 12, 65–76.

Manuscript received December 3, 1987
Manuscript accepted August 1, 1988